

# Guidance and Control Techniques for Automated Air Traffic Control

HOMER Q. LEE,\* JOHN D. MCLEAN,\* AND HEINZ ERZBERGER\*  
*NASA Ames Research Center, Moffett Field, Calif.*

A guidance technique has been developed for flying an aircraft automatically along curved trajectories. The technique consists of a set of algorithms for automatically synthesizing flight profiles, i.e., the horizontal trajectory, the altitude and speed profiles, and a time sequence of commands. The flyability of the synthesized profile under wind disturbances and initial condition error is verified by closing the loop around the synthesized trajectory and flying it in a computer-simulated jet aircraft. A control law having longitudinal, lateral and heading deviation from the synthesized profile in the feedback loops is used for the simulated flight. The performance of the system is excellent, errors that are initially zero never exceed 230 ft and large initial errors are reduced rapidly. The system also behaves quite well under wind disturbance. For example, the longitudinal and lateral deviations never exceed 470 ft for a 10-knot error in estimated wind velocity. This paper presents the flight-profile synthesis algorithms, describes the control law, analyzes the overall system performance under initial errors and error in steady wind estimates, and discusses the simulation results.

## Introduction

TO provide a basis for automated air traffic control, Ames Research Center is developing a guidance technique for flying an aircraft automatically along curved trajectories. The development has three stages: 1) mathematical formulation of terminal area guidance problems that are solved manually by the pilot and the air traffic controller; 2) development of a set of efficient computer-oriented algorithms for automatically synthesizing flight profiles in terms of horizontal trajectory, speed, altitude, and a time sequence of commands suitable for input to a stability augmentation system (SAS) or a flight director; and 3) verification of the flyability of the synthesized profiles under wind disturbances and initial errors by closing the loop around the reference trajectory and flying it in a computer-simulated jet aircraft.

This paper will present the major steps in the flight-profile synthesis and describe the control law for flying the reference trajectory. Then a performance analysis of the control law under initial condition errors will be given. Finally, performance of the over-all simulated system, consisting of the guidance algorithms, the control law, SAS and aircraft dynamics will be discussed.

## Synthesis of Guidance Profile

Several terminal area guidance problems are discussed in Ref. 1 but only one of them will be presented here, the construction of a flyable three-dimensional trajectory that begins at the current aircraft position, heading, speed, and altitude, and terminates at a prescribed position, heading, speed, altitude, and time. The terminal position would be the ILS gate, and the terminal time the assigned landing slot. Such precise time-position control has been referred to as four-dimensional guidance and is proposed as an advanced air traffic control technique.

The construction of the required trajectory is divided into three problems solved in sequence. First, the horizontal trajectory is calculated with a constraint on the turning radius. Second, the length of this horizontal trajectory and the

desired flight time are used to calculate a flyable speed profile with constraints on minimum and maximum airspeed and the acceleration and deceleration of the aircraft. Third, the altitude profile is synthesized. Finally, the completely specified trajectory is arranged into a time sequence of guidance commands.

## Horizontal Guidance

The horizontal portion of the problem is one of three discussed in Ref. 1, namely, to construct a flyable trajectory between some initial position and heading, and a specified final position and heading. The specified final position can be any point on the final approach, such as the ILS gate, and the final heading is the runway heading. Solution of the horizontal guidance problem requires specification of a rule, in the form of switching diagrams for selecting a suitable flight pattern from the set given in Ref. 1. These patterns consist of the combinations of straight lines and portions of circles that give the minimum path length subject to a constraint on turning radius. The set of possible patterns, simplified by eliminating all patterns containing three or more circular arcs, is shown in Table 1. Note that all of these patterns are basically of the form turn-straight-turn, those that are not of that form being simply degenerate cases.

The initial and final conditions are represented by the coordinates of the initial point and the initial heading, and the coordinates of the final point and the final heading. For pattern assignment, these conditions can be reduced to three parameters,  $d_0$ ,  $d_f$ , and  $\Psi$  as shown in Fig. 1 where  $P_0$  and  $P_f$  are the initial and final points, the unit vectors  $\hat{n}_0$  and  $\hat{n}_f$  indicate the initial and final directions, and  $\Psi$  is the initial heading relative to the runway. We also define a set of Cartesian coordinates, with the origin at  $P_f$  having the positive  $x$  axis in the direction of  $\hat{n}_f$ , and the positive  $y$  axis orthogonal to the right. If  $\hat{n}_0$  and  $\hat{n}_f$  are not parallel or antiparallel, lines drawn through  $\hat{n}_0$  and  $\hat{n}_f$  will intersect at point  $P_\infty$ . We shall refer to these lines as the initial and final lines. The case where these lines do not intersect is the singular case, which is treated in detail in Ref. 2 and will not be discussed here.

The pattern parameters for the nonsingular case are defined as follows. The first parameter,  $\Psi$  is the smaller angle between  $\hat{n}_0$  and  $\hat{n}_f$ . We shall take the range of  $\Psi$  to be  $-\pi < \Psi < \pi$ , with positive rotations clockwise. The remaining two parameters are  $d_0$  and  $d_f$ , where  $d_0$  is the signed distance  $\overline{P_\infty P_0}$  and  $d_f$  is the signed distance  $\overline{P_\infty P_f}$ . The sign of a distance is positive if the corresponding unit vector points away from  $P_\infty$ .

Received January 13, 1972; presented as Paper 72-121 at the AIAA 10th Aerospace Sciences Meeting, San Diego, Calif., January 17-19, 1972; revision received March 29, 1972.

Index categories: Air Navigation Communication, and Traffic Control Systems; Guidance, Control and Guidance Theory.

\* Research Scientist.

Table 1 Patterns used in simplified solution

MANEUVERS	GEOMETRIC SHAPE	MANEUVERS	GEOMETRIC SHAPE
LSL		RSR	
LSR		RSL	
LS		RS	
SL		SR	
LR		RL	
L		R	
S			

SIGNIFICANCE OF SYMBOLS IN COLUMN AS FOLLOWS:  
L-LEFT TURN S-STRAIGHT FLIGHT R-RIGHT TURN

If  $X$  and  $Y$  are the coordinates of the aircraft, then it is easily shown that  $d_0 = Y/\sin\Psi$  and  $d_f = -X + Y/\tan\Psi$ . It is convenient to normalize these coordinates by using the turning radius,  $R$ , as the unit of distance, to give

$$d_0 = Y/R \sin\Psi \quad (1)$$

$$d_f = -X/R + Y/R \tan\Psi \quad (2)$$

Equations (1) and (2) are valid for all  $\Psi$  except  $\Psi = 0$  or  $\Psi = \pi$ , which correspond to the singular cases.

Now we describe how the three parameters are used to select one of the 14 patterns shown in Table 1. Each pattern is described by some combination of  $R$ ,  $S$ ,  $L$  signifying right turn, straight flight, and left turn, respectively. The five switching diagrams, having  $d_0$  and  $d_f$  as the axes and  $\Psi$  as a parameter, required to completely specify the patterns for all combinations of initial and final conditions are derived from Ref. 2. The ranges of  $\Psi$  for these diagrams are  $\Psi = 0$ ,  $0 < \Psi < \pi/2$ ,  $\Psi = \pi/2$ ,  $\Psi < \pi$ , and  $\Psi = \pi$ . It is not neces-

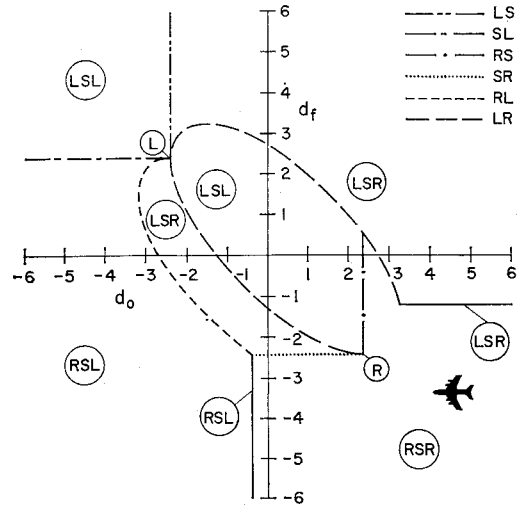


Fig. 2 Switching diagram for  $\pi/2 < \Psi < \pi$ .

sary to consider negative  $\Psi$  since the pattern for a negative  $\Psi$  is the mirror image of its positive counterpart. In other words, if the pattern for some given value of  $d_0$ ,  $d_f$ ,  $\Psi$  is RSR, then the pattern for the same value of  $d_0$ ,  $d_f$ ,  $-\Psi$  is LSL, a reflection of RSR.

A sample switching diagram for  $\pi/2 < \Psi < \pi$  is shown in Fig. 2. The curves represent boundaries between regions where one of the first four switching patterns in Table 1 is used while the lines and points represent degenerate cases as indicated on the figure. The values of  $d_0$  and  $d_f$  for a particular starting configuration determine its position on the switching diagram and, hence, the pattern used. For example, the point on the figure marked with an airplane calls for the pattern to be RSR. Each of the possible patterns has associated with it a set of pattern constants that are defined as the length of the straight line segment, its heading, and the heading changes in the initial and final turns. The equations giving those constants for the turn-straight-turn configurations are summarized in Table 2. These equations also apply to the degenerate cases if the appropriate pattern constants are set equal to zero.

The synthesis procedure may now be restated as follows: 1) compute  $\Psi$ ,  $d_0$ ,  $d_f$  from known initial position and heading and specified final position and heading, 2) for the given  $\Psi$ , locate the point  $(d_0, d_f)$  on the appropriate switching diagram to determine the flight pattern, and 3) compute the pattern constants.

### Controlled Time of Arrival

Next, we discuss the techniques used for synthesizing a speed profile that achieves the precise arrival time at the final point. Only the case of an arriving aircraft ( $V_0 > V_f$ ) is considered here, but the departure case is completely analogous and is treated in Ref. 2. The problem is generally stated as follows. Synthesize a speed profile for the given horizontal trajectory such that an aircraft, starting with initial speed  $V_0$ , arrives at the final point  $P_f$  at some specified time  $T$  with speed  $V_f$ . The constraints are that the speed  $V$  must be within the range of the minimum ( $V_{min}$ ) and maximum ( $V_{max}$ ) speed restrictions of the aircraft and that speed changes must be carried out with acceleration  $A_a$  or deceleration  $A_d$ , selected to fit the performance of a particular aircraft.

The three steps for synthesizing a controlled time of arrival profile are as follows: 1) test the feasibility of the given path length for synthesizing the speed profile and if necessary, determine a feasible path length; 2) synthesize a speed profile consisting of at most three segments, an acceleration or

Fig. 1 Pattern parameters and coordinate system.

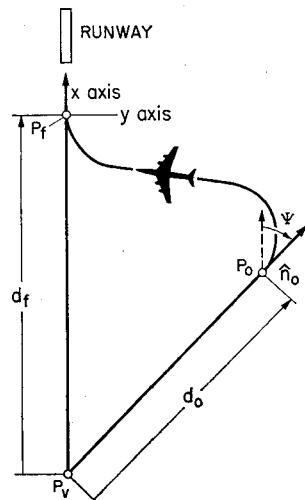


Table 2. Summary of trajectory parameter formulas

Pattern type	$\overline{P_1 P_2}$ Length of straight line segment	$\Psi_s$ Heading of straight line segment	$\Psi_1$ Heading change in initial turn	$\Psi_2$ Heading change in final turn
RSR	$[(X - R \sin \Psi)^2 + (R - R \cos \Psi - Y)^2]^{1/2}$	$\arctan \frac{R - R \cos \Psi - Y}{-X + R \sin \Psi}$	$\Psi_i = \begin{cases} \Psi_s - \Psi; \Psi_s \geq \Psi \\ \Psi_s + 2\pi - \Psi; \Psi_s < \Psi \end{cases}$	$\Psi_f = \begin{cases} 2\pi - \Psi_s; \Psi_s > 0 \\ 0; \Psi_s = 0 \end{cases}$
RSL	$\frac{2R}{\tan \Psi'}$ where $\Psi' = \arcsin \frac{2R}{[(X + R \sin \Psi)^2 + (R + R \cos \Psi + Y)^2]^{1/2}}$	$\Psi_s = \begin{cases} \Psi_1 + \Psi'; \Psi_1 + \Psi' < 2\pi \\ \Psi_1 + \Psi' - 2\pi; \Psi_1 + \Psi' \geq 2\pi \end{cases}$ where $\Psi_1 = \arctan \frac{-R - R \cos \Psi - Y}{-X + R \sin \Psi}$	$\Psi_i = \begin{cases} \Psi_s - \Psi; \Psi_s \geq \Psi \\ \Psi_s + 2\pi - \Psi; \Psi_s < \Psi \end{cases}$	$\Psi_f = \Psi_s$
LSL	$[(X + R \sin \Psi)^2 + (R - R \cos \Psi - Y)^2]^{1/2}$	$\arctan \frac{-R + R \cos \Psi - Y}{-X - R \sin \Psi}$	$\Psi_i = \begin{cases} \Psi - \Psi_s; \Psi \geq \Psi_s \\ \Psi - \Psi_s + 2\pi; \Psi < \Psi_s \end{cases}$	$\Psi_f = \Psi_s$
LSR	$\frac{2R}{\tan \Psi'}$ where $\Psi' = \arcsin \frac{2R}{[(X + R \sin \Psi)^2 + (R + R \cos \Psi - Y)^2]^{1/2}}$	$\Psi_s = \begin{cases} \Psi_1 - \Psi'; \Psi_1 - \Psi' \geq 0 \\ \Psi_1 - \Psi + 2\pi; \Psi_1 - \Psi' < 0 \end{cases}$ where $\Psi_1 = \arctan \frac{R + R \cos \Psi - Y}{-X - R \sin \Psi}$	$\Psi_i = \begin{cases} \Psi - \Psi_s; \Psi \geq \Psi_s \\ \Psi - \Psi_s + 2\pi; \Psi < \Psi_s \end{cases}$	$\Psi_f = \begin{cases} 2\pi - \Psi_s; \Psi_s > 0 \\ 0; \Psi_s = 0 \end{cases}$

deceleration segment starting at  $V_0$ , a constant speed segment at some speed  $V_n$ , and another acceleration or deceleration segment ending at  $V_f$ ; and 3) determine the numerical values of the speed and times that completely specify the profile.

To test the feasibility of the path length, it is compared with  $L_{\max}$  and  $L_{\min}$ , which are the maximum and minimum distances the aircraft is capable of traversing during the allotted time, respectively. If the path length exceeds  $L_{\max}$ , the speed profile is beyond the aircraft's performance capability of flying, and a later arrival time must be specified. If the path length is less than  $L_{\min}$ , it must be increased so that the new path length is within the range of  $L_{\min}$  to  $L_{\max}$  (a technique for increasing the path length is presented in Ref. 2). The feasible path length will be denoted by  $L$ .

Let  $L_1$  and  $L_2$  be, respectively, the minimum and maximum distances that can be traversed in the allotted time interval if the speed is constrained to lie between  $V_0$  and  $V_f$ . The parameters  $L_1$  and  $L_2$ , which correspond to the shaded areas in Fig. 3a, are used to select the speed profile for  $L$  from those in Fig. 3b. For example if  $L$  is less than  $L_1$ , the profile labelled  $d-c-a$  is used where  $a$ ,  $c$ , and  $d$  stand for acceleration, constant speed, and deceleration, respectively. If  $L > L_2$ , profile  $a-c-d$  is used, while for  $L_1 > L > L_2$ , the profile is  $d-c-d$ . The equations for  $L_1$ ,  $L_2$ ,  $L_{\min}$ , and  $L_{\max}$  are

$$L_1 = V_f T + (V_0 - V_f)^2 / 2 |A_d| \quad (3)$$

$$L_2 = V_0 T - (V_0 - V_f)^2 / 2 |A_d| \quad (4)$$

$$L_{\min} = V_{\min} T + (V_0 - V_{\min})^2 / 2 |A_d| + (V_{\min} - V_f)^2 / 2 A_a \quad (5)$$

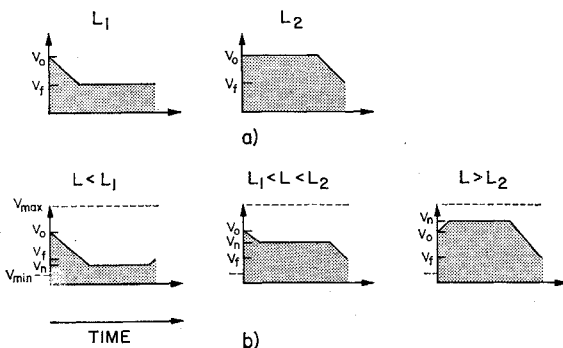


Fig. 3 Profile for speed control.

$$L_{\max} = V_{\max} T - (V_{\max} - V_0)^2 / 2 A_a - (V_{\max} - V_f)^2 / 2 |A_d| \quad (6)$$

The numerical value of the constant speed  $V_n$  is determined by matching the area under the synthesized speed curve to the feasible path length  $L$ . The remaining constants needed to completely specify the speed profile are  $t_1$  and  $t_2$ , the times corresponding to the beginning and termination of the constant speed segment. If the rates of change of speed in the first and third segments are  $a_1$  and  $a_3$ , respectively, then the numerical values of  $V_n$ ,  $t_1$ , and  $t_2$  may now be computed by the following relations:

$$V_n^2 \left( \frac{1}{2a_3} - \frac{1}{2a_1} \right) + V_n \left( T + \frac{V_0}{a_1} - \frac{V_f}{a_3} \right) + \left( \frac{V_f^2}{2a_3} - \frac{V_0^2}{2a_1} - L \right) = 0 \quad (7)$$

$$t_1 = V_n - V_0 / a_1 \quad (8)$$

$$t_2 = T - V_f - V_n / a_3 \quad (9)$$

For the profile to be physically meaningful  $t_1 \leq t_2$ , but the above equations are also valid for the degenerate cases of one or two segments.

### Vertical Guidance

The only information required to define the vertical profile is the time to begin the descent to the desired final altitude. For simplicity it will be assumed that descent will occur at the latest possible time, but other criteria might be used. This time is calculated by subtracting from the specified arrival time  $T$  the time interval required to make the speed change from the  $V_n$  speed to the specified final speed in level flight and the time interval required to change the altitude from cruise altitude to final altitude. The first time interval is available from the speed-time history already calculated; the second interval is given by the relation  $(h_c - h_f)/h$ , where  $h_c$ ,  $h_f$ , and  $h$  are cruising altitude, final altitude, and rate of altitude change, respectively.

### Over-All Flight Profile and Example

We will use a numerical example to illustrate the synthesis of a three-dimensional trajectory with time constraints by the techniques just discussed. Consider an aircraft whose current

position is 8 miles from the *ILS* gate, at an azimuth of  $292^\circ$ . It has a heading of  $216^\circ$ , an altitude of 3000 ft, and a speed of 189.6 knots. The flight profile to be synthesized is to guide the aircraft to arrive at the gate 4 min later, aligned with the runway at the final altitude of 1500 ft and a final speed of 130 knots. The acceleration and deceleration capability of the aircraft is  $1 \text{ fps}^2$  and the maximum and minimum speeds of the aircraft are 300 and 130 knots, respectively. The sink rate (the rate of change of altitude) is 1000 ft/min. The aircraft is to maintain cruise altitude (3000 ft in this case) as long as possible, to descend at constant speed and to hold altitude during speed changes. A turning radius of 2 miles is to be used during horizontal maneuvers.

To synthesize the horizontal trajectory, the pattern parameters  $d_o$ ,  $d_f$  are found to be 6.3097 and  $-6.6031$  by using Eqs. (1) and (2), respectively. These are the coordinates of the airplane shown in Fig. 1. The flight pattern is RSR according to the switching diagram, but since heading modulus  $180^\circ$  is  $-144^\circ$  a reflection about the  $d_o$  axis is required giving *LSL* as the pattern to be used. The turning angles  $\Psi_i$  and  $\Psi_f$ , linear path  $P_1P_2$ , and total path length  $l$ , all computed by using the equations for the *LSL* pattern in Table 2, are  $100.389^\circ$ ,  $115.611^\circ$ , 3.5042 miles, and 11.75 miles, respectively.

The minimum and maximum path length  $L_{\min}$  and  $L_{\max}$  are computed from Eqs. (5) and (6) and are 14.51 and 10.93 miles, respectively. Since the given horizontal path length is 11.75 miles, it is within the range of feasible path length and is therefore the path length  $L$ . The distances  $L_1$  and  $L_2$  are computed by substituting numerical values into Eqs. (3) and (4), and are 10.93 and 13.58 miles, respectively. Since  $L$  is greater than  $L_1$  and less than  $L_2$ , and  $V_o$  is greater than  $V_f$ ,  $d-c-d$  is the shape of the required speed profile (Fig. 3). The values of  $V_n$ ,  $t_1$ , and  $t_2$  (250.54 fps, 69.46 sec, and 208.88 sec, respectively) are computed by substituting the numerical values of  $a_1$ ,  $a_3$ ,  $V_o$ ,  $V_f$ ,  $T$ , and  $L$  into Eqs. (7, 8, and 9).

The time duration  $\Delta t_h$  required to descend from a cruising altitude of 3000 ft to a final altitude of 1500 ft at a sink rate of 1000 ft/min is 90 sec. Since the aircraft is required to descend only when the speed is constant, descending can only take place within the time interval [64.46, 208.88] seconds. Since the duration of this time interval is 139.42 sec and is greater than  $\Delta t_h$ , it is possible to descend at constant speed. The aircraft is also required to maintain cruise altitude as long as possible so that altitude change will take place during the last portion of the constant-speed time interval, from 118.88 sec to  $t_2$ .

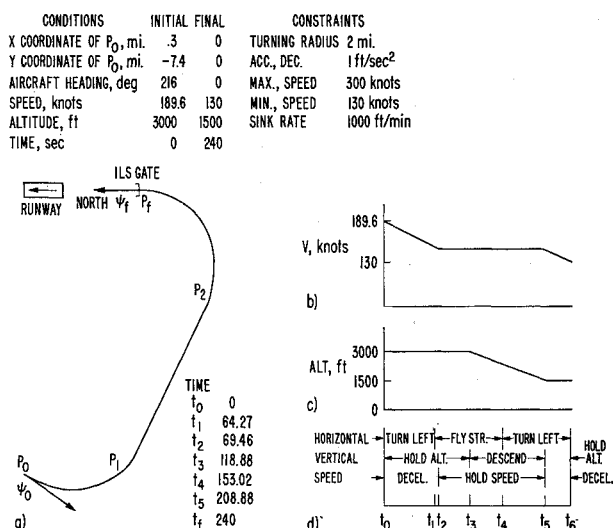


Fig. 4 Over-all flight profile.

The time command sequence specifies the commands, time instants of initiation, and termination of commands required to fly the profile. To synthesize the over-all command profile it is necessary to express the horizontal guidance, controlled time of arrival, and altitude profile in a time sequence. The times for termination of the first left turn and for initiation of the second left turn are obtained by determining the time required to traverse the arc lengths  $P_0P_1$  and  $P_2P_f$ , respectively. Their numerical values are 64.27 and 153.02 sec, respectively. A complete command profile can now be constructed from a time history of the three profiles. For convenience the subscripts are renamed in the order of the command to be executed, i.e., left turn, decelerate, descend, etc.

Figure 4 is a complete profile of the over-all trajectory. The profile includes a horizontal trajectory, speed, altitude, and command-sequence history.

### Perturbation Equations and Control Law

Having developed a synthesis procedure for the over-all flight profile, which we will now refer to as the reference trajectory, the next step is to design a control law for flying it. The design of a control law for a similar problem, that of guiding a helicopter along a curved trajectory was studied by Hoffman et al.<sup>3</sup> The method of design used here is more flexible in that it permits the control of aircraft along a more general class of trajectory. As in Ref. 3, the design is accomplished by means of a perturbation method. Design of the control law for the altitude channel will not be considered here since this channel is simple with minimal coupling to the other channels. The method used to derive the remainder of the control law is described next.

The nonlinear dynamical equations, from which the perturbation equations are derived, are as follows,

$$\dot{X} = V \cos \Psi \quad (10)$$

$$\dot{Y} = V \sin \Psi \quad (11)$$

$$\dot{\Psi} = g/V \tan \Phi \quad (12)$$

where  $V$  is the ground speed,  $\dot{X}$ ,  $\dot{Y}$  are components of  $V$ ,  $\Psi$  is the ground heading,  $\dot{\Psi}$  the heading rate,  $\Phi$  the bank angle, and  $g$  acceleration of gravity. The wind is assumed to be zero. The aircraft's position coordinates,  $X$ ,  $Y$ , heading  $\Psi$ , speed  $V$ , and bank angle  $\Phi$  are related to the reference  $X_r$ ,  $Y_r$ ,  $\Psi_r$ ,  $V_r$ , and  $\Phi_r$  as follows,

$$X = X_r + \Delta X \quad (13)$$

$$Y = Y_r + \Delta Y \quad (14)$$

$$\Psi = \Psi_r + \Delta \Psi \quad (15)$$

$$V = V_r + \Delta V \quad (16)$$

$$\Phi = \Phi_r + \Delta \Phi \quad (17)$$

where  $\Delta X$ ,  $\Delta Y$ ,  $\Delta \Psi$ ,  $\Delta V$  and  $\Delta \Phi$  are perturbed quantities. The dynamical equations for  $\Delta X$ ,  $\Delta Y$  and  $\Delta \Psi$ , obtained by substituting Eqs. (13–17) and their derivatives into Eqs. (10–12) and by using a Taylor series expansion about the reference quantities, are

$$\Delta \dot{X} = -V_r \sin \Psi_r \Delta \Psi + \cos \Psi_r \Delta V \quad (18)$$

$$\Delta \dot{Y} = V_r \cos \Psi_r \Delta \Psi + \sin \Psi_r \Delta V \quad (19)$$

$$\Delta \dot{\Psi} = g/V_r \sec^2 \Phi_r \Delta \Phi - \Delta V/V_r \Psi_r \quad (20)$$

To eliminate the  $\sin \Psi_r$  and  $\cos \Psi_r$  terms,  $\Delta X$  and  $\Delta Y$  are transformed into a moving target reference system by the following relations,

$$\begin{pmatrix} x \\ y \end{pmatrix} = \begin{pmatrix} \cos \Psi_r & \sin \Psi_r \\ -\sin \Psi_r & \cos \Psi_r \end{pmatrix} \begin{pmatrix} \Delta X \\ \Delta Y \end{pmatrix} \quad (21)$$

$$\dot{\psi} = \dot{\Psi} - \dot{\Psi}_r \quad (22)$$

Differentiating Eq. (21) and substituting into Eqs. (18) and (19) give

$$\dot{x} = v + \dot{\Psi}_r y \quad (23)$$

$$\dot{y} = V_r \psi - \dot{\Psi}_r x \quad (24)$$

where  $v = \Delta V$ ,  $\varphi = \Delta \Phi$ , and  $\psi = \Delta \Psi$ . Equation (20) may be expressed in terms of  $v$ , and  $\varphi$  as follows:

$$\dot{\psi} = (g/V_r) \sec^2 \Phi_r \varphi - (\dot{\Psi}_r/V_r) v \quad (25)$$

The moving target reference system is illustrated in Fig. 5. The origin and positive  $x$ -axis of this moving target reference system at any given time are the reference position and the direction of the ideal aircraft flying the reference trajectory, respectively. The advantage of using this system is that the dependence of the control law on the reference trajectory becomes greatly diminished. Furthermore, since the coordinates and heading of the aircraft expressed in this system are position and heading error, the control objective is to null these quantities. Equations (23) and (24) show that the dynamical equations for  $x$  and  $y$  are coupled by  $\dot{\Psi}_r$ , except when  $\dot{\Psi}_r$  is zero, while the gain of the  $\psi$  channel is inversely proportional to the reference speed  $V_r$ , so that  $\dot{\Psi}_r$  and  $V_r$  are parameters in the perturbation equation.

The control variables of the aircraft for horizontal maneuver are the bank angle  $\Phi$  and the speed  $V$ . A linear model of the combined autopilot and aircraft dynamical response for a bank angle and velocity command system can be approximated by the following equation

$$\ddot{\varphi} = (1/\tau_\varphi)(-\dot{\varphi} + K_\varphi \varphi - K_\varphi \varphi_{fb}) \quad (26)$$

$$\ddot{v} = (1/\tau_v)(-\dot{v} + K_v v - K_v v_{fb}) \quad (27)$$

where  $\varphi_{fb}$  and  $v_{fb}$  are the command inputs and  $\varphi$  and  $v$  are the response. The parameters in these two equations,  $K_\varphi$ ,  $K_v$ ,  $\tau_\varphi$ ,  $\tau_v$ , were deduced by matching the time histories of these equations to those of a currently in-service, 4-engine, jet-aircraft with an autopilot and auto-throttle. Their numerical values are  $0.375 \text{ sec}^{-1}$ ,  $0.167 \text{ sec}^{-1}$ ,  $1.04 \text{ sec}$ , and  $4.17 \text{ sec}$ , respectively. The following control law is chosen for nulling the perturbed quantities  $x$ ,  $y$ , and  $\psi$

$$\varphi_{fb} = -k_{\varphi y} y - k_{\varphi \psi} V_r \psi + k_{\varphi x} \dot{\Psi}_r x \quad (28)$$

$$v_{fb} = -k_{v x} x - k_{v y} \dot{\Psi}_r y \quad (29)$$

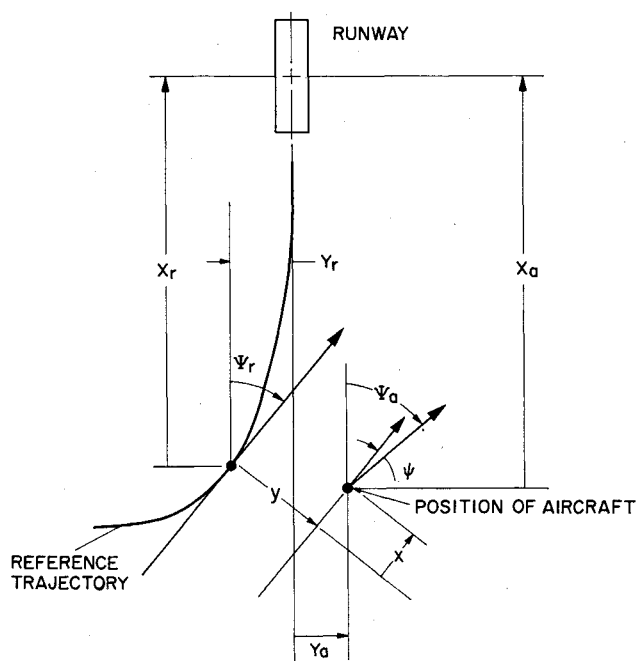


Fig. 5 Moving target reference systems.

Note that the feedback law contains  $\dot{\Psi}_r$  and  $V_r$  as parameters. The purpose of this parametrization is to obtain a feedback law which is applicable to a wide variety of reference trajectories. Combining Eqs. (23–29), in matrix form gives

$$\dot{x} = Fx \quad (30)$$

where  $x$  is the state vector, having  $x$ ,  $v$ ,  $\dot{v}$ ,  $y$ ,  $\psi$ ,  $\varphi$  and  $\dot{\varphi}$  as its components. The eigenvalues of the matrix  $F$  are the poles of the closed-loop system, linearized about some fixed reference speed  $V_r$  and reference heading rate  $\dot{\Psi}_r$  (or equivalently a fixed bank angle since  $\dot{\Psi}_r = (g/V_r) \tan \Phi_r$ ).

The governing factors for determining the numerical values of the five gains  $k_{vx}$ ,  $k_{vy}$ ,  $k_{\varphi x}$ ,  $k_{\varphi y}$ , and  $k_{\varphi \psi}$  are; a) the accuracy of the navigation data, b) the allowable bank angle and throttle activity for passenger comfort, and c) the accuracy of following the synthesized reference trajectory. Application of a criterion for determining the optimal feedback gains are currently being investigated. However, a preliminary eigenvalue analysis indicates that a good compromise between conflicting requirements b) and c) is to use  $0.000186 \text{ rad/ft}$  for  $k_{\varphi y}$ ,  $0.003863 \text{ rad/rad (fps)}$  for  $k_{\varphi \psi}$ ,  $0.0001 \text{ rad/ft (rad/sec)}$  for  $k_{\varphi x}$ ,  $0.0444 \text{ (fps)/ft}$  for  $k_{vx}$ , and  $0.15 \text{ (fps)/ft (rad/sec)}$  for  $k_{vy}$ . This combination of gain constants was obtained by trial and error using root-locus analysis of Eq. (30).

The eigenvalues corresponding to this set of gains yield reasonable frequency and damping. Figure 6 shows 3 branches of the root locus plot for this set of gains as a function of  $\dot{\Psi}_r$ , ranging from  $0^\circ/\text{sec}$  to  $6^\circ/\text{sec}$ . Not shown in the figure are their complex conjugates and another pair of well-damped complex poles whose location is insensitive  $\dot{\Psi}_r$  changes. This accounts for all 7 poles of matrix  $F$ . The dashed and solid lines are root loci of a system with and without the cross feedback gains  $k_{\varphi x}$  and  $k_{vy}$ . At  $\dot{\Psi}_r = 0^\circ/\text{sec}$ , the damping ratio for the upper and lower branches are  $0.52$  and  $0.86$  respectively. At  $\dot{\Psi}_r = 6^\circ/\text{sec}$ , the damping ratio for the upper branch is  $0.23$  for a system with cross feedback and  $0.15$  for a system without cross feedback, and for the lower branch,

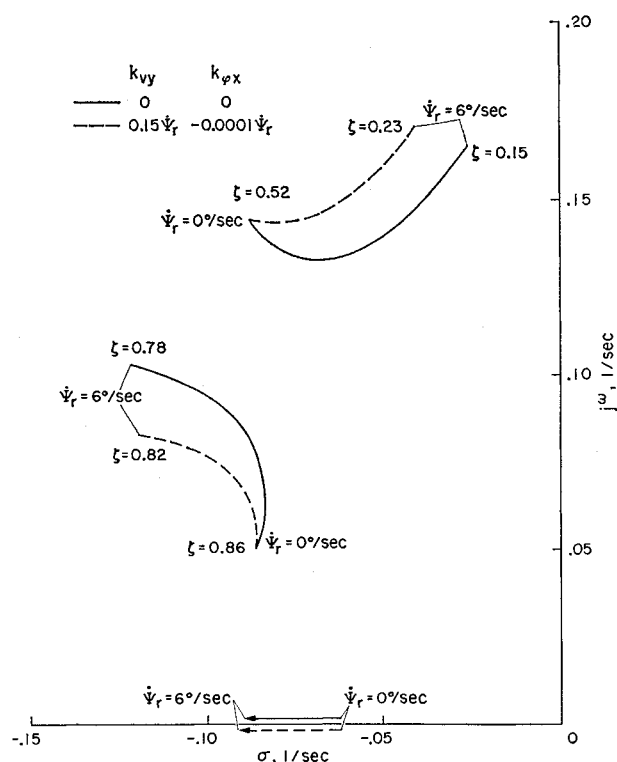


Fig. 6 Root locus of linearized system.

it is 0.82 for the system with cross feedback and 0.78 for the system without cross feedback. The root loci illustrate a definite improvement on system stability by using cross feedback.

It is to be emphasized that all feedback gains are constants and their pole location, indicated in the figure, are the best compromise achievable between system stability and minimal autopilot and auto-throttle activity. An eigenvalue search shows that the damping ratio for the upper branch can be increased for nonzero value of  $\Psi_r$  by allowing  $k_{vx}$  to change as a function of  $\Psi_r$ . However, this increase in stability can only be accomplished at the expense of some slight reduction in the damping ratio of the lower branch.

### Simulation Results

The guidance technique and the control law described in previous sections were evaluated in a computer-simulated flight of a jet-aircraft. Figure 7 shows a block diagram of the

simulation. Major elements in the diagram are the "Trajectory Synthesis and Guidance" algorithms, the "Control Law" and the "Aircraft Autopilot and Kinematics." The last element includes the effect of wind and the limits on bank angle, bank angle rate, acceleration, vertical rate and vertical acceleration.

The simulation results for the example reference trajectory (given in the previous section) are shown in Fig. 8 as error time history plots. The performance of the system is excellent; the errors that are initially zero never exceed 230 ft while the large initial errors of the other case are reduced quite rapidly. Note that in the moving target reference coordinate system, the  $x$  and  $y$  errors are completely interchanged after a  $90^\circ$  turn in the reference trajectory. This explains the very rapid reduction in  $x$  error at the expense of some build up in  $y$  error. The response of the system to errors in the estimated wind velocity was also investigated. It was found that a 10-knot wind in opposite direction to the final heading resulted in errors that did not exceed 350 and 470 ft in  $x$  and  $y$ , respectively.

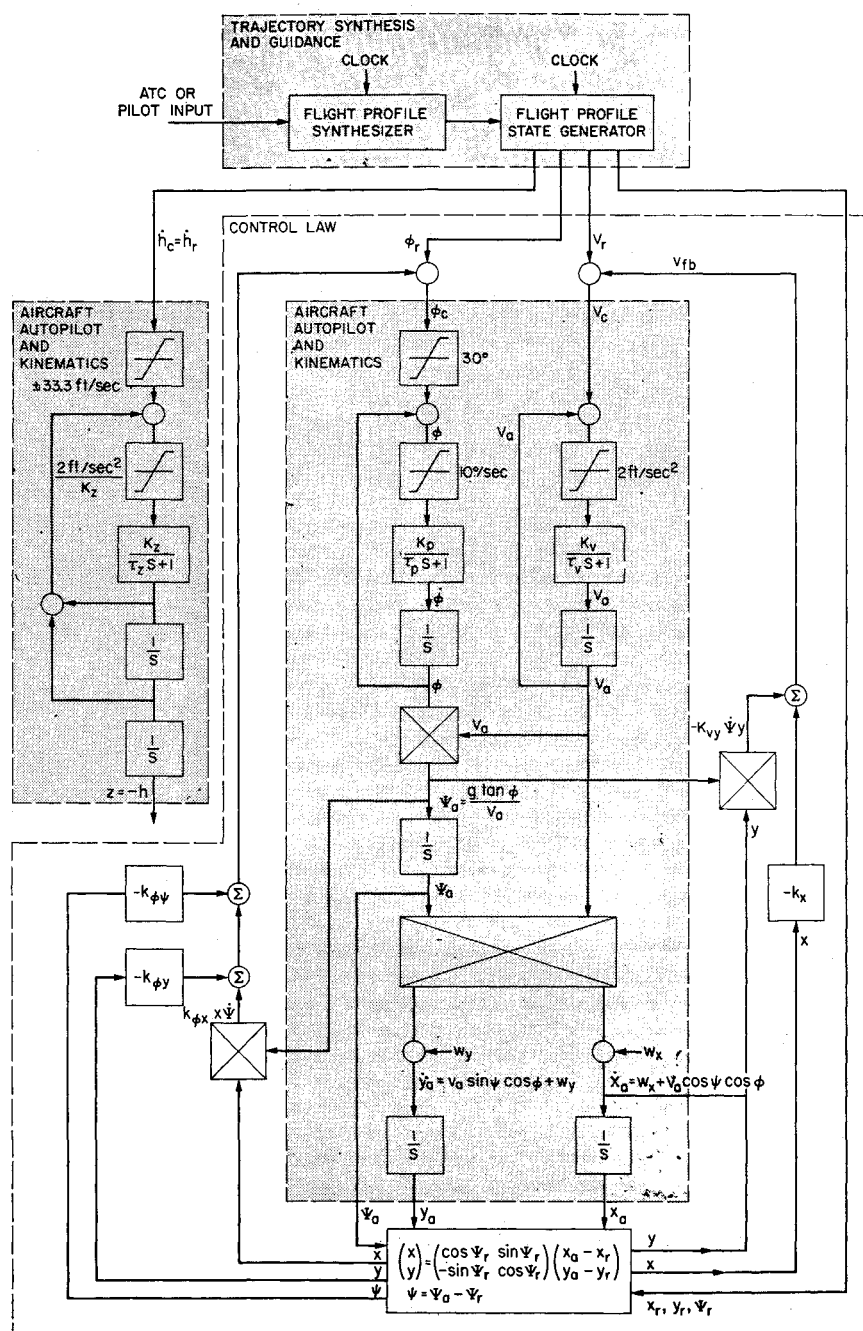


Fig. 7 Block diagram of simulated aircraft and control law.

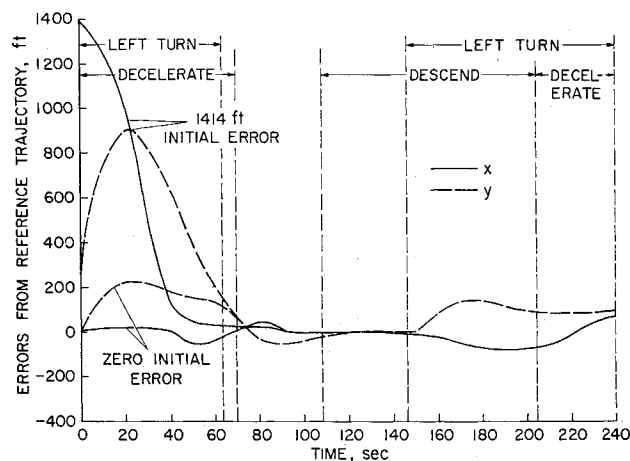


Fig. 8 Time histories of errors in following reference trajectory.

This control law was also used in a simulated flight of STOL type trajectory (see Fig. 9). The reference speed for this trajectory is 135 fps and the turning radius is 1220 ft. This value of speed and turning radius demands almost maximum bank, leaving only little bank margin for nulling out errors. The initial  $y$  error is one half turning radius and the magnitude and direction of the error were so chosen that the aircraft is prevented from achieving the commanded bank angle by the bank angle limits. The resulting time histories plot is shown

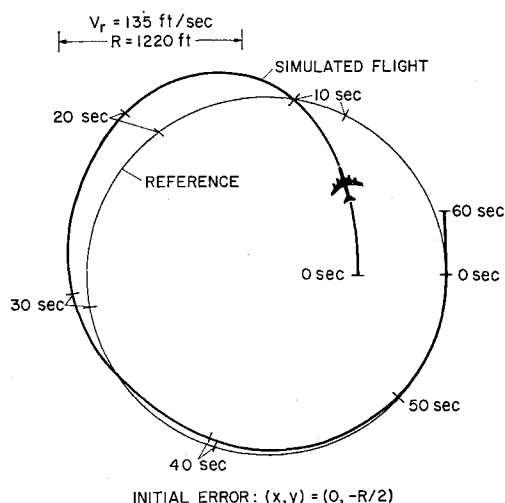


Fig. 9 Simulated STOL trajectory.

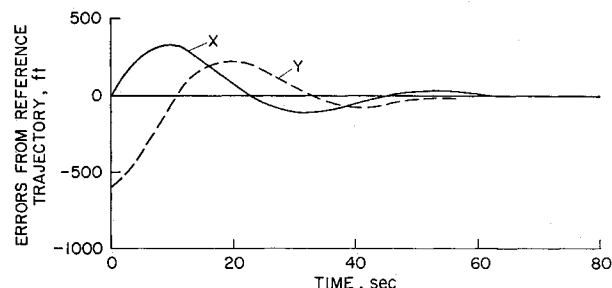


Fig. 10 Time histories of errors in following STOL trajectory.

in Fig. 10. The initial error is reduced quite rapidly and the aircraft begins to lock onto the reference trajectory about 50 sec later.

## Conclusion

In general, the over-all flight profile of an aircraft, starting from takeoff to landing, can be decomposed into a sequence of waypoints. The flight profile for each pair of adjacent waypoints can readily be synthesized by the application of the guidance technique presented here. Therefore, the over-all flight profile from takeoff to landing may be synthesized by concatenation of flight profiles for consecutive pairs of waypoints.

The advantage of this technique lies in its versatility and efficiency. It requires no precomputation of trajectories and it makes provision for fast in-flight changes in trajectory should they be required. Since the only aircraft parameters used in synthesizing the trajectories are performance limitations, which are treated as parameters, the technique is applicable to any aircraft. By synthesizing trajectories subject only to aircraft performance limitations and ATC constraints, the technique uses airspace efficiently, and therefore, should make it possible to reduce separation requirements and thus, achieve higher landing rates.

## References

- Erzberger, H. and Lee, H. Q., "Optimum Horizontal Guidance Techniques for Aircraft," *Journal of Aircraft*, Vol. 8, No. 2, Feb. 1971, pp. 95-101.
- Erzberger, H. and Lee, H. Q., "Terminal Area Guidance Algorithms for Automated Air Traffic Control," TN D-6773, 1972, NASA.
- Hoffman, W. C., Zvara, J., Bryson, A. E. Jr., and Ham, N. D., "Automatic Guidance Concept for VTOL Aircraft," *Journal of Aircraft*, Vol. 8, No. 8, Aug. 1971, pp. 637-642.